Numerical modeling of sea ice in the climate system

by Cecilia M. Bitz
Atmospheric Sciences, University of Washington

Worldwide emissions of CO_2 from human energy-related activities are currently about 30 billion metric tons per year (a metric ton is 10^3 kg). One outcome of the resulting rise in anthropogenic CO_2 levels has been a growing concern for the loss of ice and snow in the polar regions. The loss of ice and snow changes the way of life for humans, plants, and animals and amplifies the climate response in the Arctic. The global warming problem motivates many to understand and model the physics of sea ice. There are many other worthwhile reasons as well.

This chapter is a compilation of two lectures I presented at the IPY Sea Ice Summer School in Svalbard, July 2008. Part one is about how sea ice is modeled in the leading global climate models, and part two is a guide to the sea ice thermodynamic modeling exercises that I led at the summer school.

I will begin part one with a brief history of sea ice modeling in climate models. Next, I will lay out the highest level governing equations for a state of the art climate model and describe their implementation in words and pictures. My intention is to explain why I think certain physics is important and how it affects the climate model behavior. I will not do justice to the topic of sea ice dynamics, not because it is unimportant, but because this topic has been taken up by others in this volume. I will describe some general considerations about numerical and computational considerations for these models. I will conclude with suggestions about where I think efforts should be focused to further improve sea ice models. I hope to make the case that computation expense is a poor excuse for putting off many model improvements.

The modeling exercises in part two use a one-dimensional thermodynamic sea ice model with explicit brine-pocket physics that has been used in several global climate models. The exercises are designed to investigate the role of sea ice in the climate system and issues that global climate modelers face when developing a sea ice model.

1 Modeling Sea ice in Global Climate Models

1.1 A Brief History

Although the basic influence of sea ice on polar climate has been understood for a half-century or more (e.g., Untersteiner, 1961; Fletcher, 1965), the sea ice components of climate models lagged behind other components of climate models in the 20th century. I believe this is because the main importance of sea ice was thought to be its role in ice-albedo feedback (see, e.g., Shine et al., 1984). Until the last decade or so, sea ice albedo measurements on a local scale were scarce, and none existed on a climate model gridscale. With little basis for designing a realistic albedo parameterization prior to the 1990s, modeling centers kept the

whole sea ice component as simple as possible and directed their limited human resources elsewhere.

The earliest "global climate models" were energy balance models, such as the Budyko and Sellers type (Budyko, 1969; Sellers, 1969). These models accounted for ice-albedo feedback by parameterizing the ocean surface albedo as a function of sea surface temperature. Thus sea ice was essentially modeled as an ocean painted white. The albedo difference between blue and white ocean areas determined the strength of the polar amplification. Anyone who has run this kind of climate model quickly discovers that the polar climate and polar amplification varies radically depending on this albedo difference.

Implementing a realistic albedo parameterization is just one step in writing a good sea ice model. The albedo parameterization is only ever as good as the success of modeling the sea ice basic state — the ice-thickness distribution, ice motion, snow depth, melt-pond coverage, etc. A simple sea ice model, for example, one that assumes a fixed pond coverage and/or lead fraction in summer has fewer degrees of freedom and perhaps less can go wrong. Furthermore, a simple model takes fewer computational resources, is easier to tune (adjustments made to model parameters to produce a reasonable sea ice cover), and tends to be more robust in the face of biases in other components. It would also seem that some of the poor physics in the sea ice component of global climate models defies reason.

Basin-scale models that treat the sea ice as a viscous-plastic (VP) material and another that also explicitly modeled the ice-thickness distribution (ITD), both still in common use today, were developed and demonstrated decades ago by Hibler (1979, 1980). Sea ice thermodynamics that took into account the thermal inertia of brine-pocket physics was developed by Untersteiner (1961) and Maykut and Untersteiner (1971). However, climate modelers thought these methods were too complex and computationally demanding to be implemented until decades after their invention. Instead as climate models developed in the 1980 and early 1990s, they implemented primitive equation atmosphere and ocean models, but often treated sea ice as a uniform slab without brine pockets or melt ponds (see Table 1). Some allowed the sea ice to move but usually only in free drift, with no internal ice force.

It wasn't until Flato and Hibler (1992) simplified the VP model by treating sea ice as a cavitating fluid (CF) that global climate modelers attempted to implement sea ice dynamics with a constitutive law (with an internal ice force). Then Hunke and Dukowicz (1997) developed a technique of treating sea ice as an elastic-viscous-plastic (EVP) material — a numerical approximation to the VP model that asymptotes to the full VP solution and yet is efficient, highly parallelizable, and offers flexible grid choices. Zhang and Hibler (1997) followed suit by making the VP numerics more efficient and parallelizable. These new dynamical schemes ushered in a time of rapid improvement in the sea ice dynamics in climate models, and now EVP and VP dynamics are in wide use among climate models.

Methods to treat sea ice thermodynamics were also evolving. The thermodynamic model of Maykut and Untersteiner (1971) was adapted for climate modeling and taken a step further to account for brine pockets in the sea ice enthalpy by Bitz and Lipscomb (1999). Their thermodynamic scheme was demonstrated in a global climate model with a Lagrangian ice-thickness distribution (Bitz et al., 2001). The thermodynamics of Bitz and Lipscomb (1999) was subsequently simplified to only allow brine pocket physics in the upper layer by Winton (2000). A refinement to the numerics of the Lagrangian ice-thickness distribution improved

its accuracy (Lipscomb, 2001).

Table 1: Sea ice physics in models participating in phase two of the Coupled Model Intercomparison Project (CMIP2, Meehl et al., 2000), which had a target deadline for submitting data by April 1997. Based on table 1 from Holland and Bitz (2003) with original information from references cited there. Some references did not completely describe the sea ice component, which lead to missing information in the table below. All models include basic thermodynamics, but no information about the number of temperature layers was available.

Modeling Center	Abbrev.	Sea Ice Physics[1]
Bureau of Meteorology Research Center (Australia)	BMRC	no dynamics, no leads
Canadian Centre for Climate Modelling and Analysis	CCC	no dynamics, leads
Center for Climate System Research (Japan)	CCSR	no dynamics, no leads
Centre Europeen de Recherche et de Formation Avancee en Calcul Scientifique (France)	CERF	no dynamics, statistical ITD
Commonwealth Scientific and Industrial Research Organization (Australia)	CSIRO	CF, leads
National Center for Atmospheric Research (USA)	CSM	CF, leads
Max-Planck-Institut fuer Meteorologie (ECHAM3+LSG Model) (Germany)	ECH3	no dynamics, no leads
Geophysical Fluid Dynamics Laboratory (USA)	GFDL	FD, no leads
Goddard Institute for Space Studies (USA)	GISS	CF, leads
United Kingdom Meteorological Office	HadCM3	FD, leads
Meteorological Research Institute (Japan)	MRI	FD
Department of Energy (USA)	PCM	EVP, leads

[1]CF = Cavitating Fluid dynamics, ITD = Ice-Thickness Distribution, EVP = Elastic-Viscous Plastic dynamics, and FD = Free Drift dynamics (neglects the internal ice force).

During this golden-age of global climate model development, field projects such as SHEBA and ASPeCt offered improved and more complete measurements of the sea ice albedo (Perovich and Coauthers, 1999; Brandt et al., 2005) and many other properties that are important for modeling sea ice. With the help of these data, there have been concerted efforts to improve many sea ice parameterizations in global climate models.

The evolution of sea ice physics in global climate models can be seen in two intercomparison projects summarized in Tables 1 and 2. With only 7 years between intercomparison projects, the sea ice physics made marked advances. Less than 1/4 of the earlier models had sea ice dynamics, and most that did used CF dynamics. In contrast, nearly all of the later models have EVP or VP dynamics and about 1/4 also have an ITD. About half of the later models resolved a vertical temperature profile and some even parameterize brine-pockets.

To my knowledge none of the models listed in tables 1 and 2 include explicit melt ponds or two-stream radiative transfer in the ice. Some attept to approximate the behavior of melt ponds with a temperature dependent surface albedo for bare ice conditions. The models that have two or more ice layers usually have some internal solar absorption, sometimes via a heat reservoir, as in Semtner (1976). Others, at best, use Beer's law to let the solar radiation

Table 2: List of models participating in CMIP3 (Meehl et al., 2007), which had a target deadline for submitting data by September 2004. Based on information given by the modeling centers at http://www-pcmdi.llnl.gov/ipcc/model_documentation/ipcc_model_documentation.php, which was sometimes incomplete and may lead to missing information in the table below. All models have basic thermodynamics and leads.

Modeling Center	Abbrev.	Sea Ice Physics[1]
Bjerknes Centre for Climate Research (Norway)	BCCR	VP, 0 layers
Canadian Centre for Climate Modelling and Analysis	CGCM3.1	CF, 0 layers
Météo-France/Centre National de Recherches Météorologiques	CNRM-CM3	ITD, EVP 4 layers
National Center for Atmospheric Research (USA)	CCSM3	ITD, EVP, 4 layers, brine pockets
Commonwealth Scientific and Industrial Research Organization (Australia)	CSIRO-Mk3.5	CF, 3 layer, heat reservoir
Max Planck Institute for Meteorology (Germany)	ECHAM5-MPI	VP, 0 layers
Meteorological Institute of the University of Bonn, Meteorological Research Institute of KMA, and Model and Data group (Germany/Korea)	ECHO-G	VP, 0 layers
LASG / Institute of Atmospheric Physics (China)	FGOALS-g1.0	ITD, EVP, 16 layers
Geophysical Fluid Dynamics Laboratory (USA)	GFDL-CM2.1	ITD, EVP, 3 layers, brine pockets
Goddard Institute for Space Studies (USA)	GISS-AOM	CF, 4 layers
Goddard Institute for Space Studies (USA)	GISS-ER	VP, 4 layers
United Kingdom Meteorological Office	HadCM3	FD, leads 0 layers
United Kingdom Meteorological Office	HadGEM1	ITD, EVP, 0 layers
Institute for Numerical Mathematics (Russia)	INM-CM3.0	No dynamics, 0 layers
Institut Pierre Simon Laplace (France)	IPSL-CM4	VP, 3 layers, heat reservoir
Center for Climate System Research, National Institute for Environmental Studies, and Frontier Research Center for Global Change (Japan)	MIROC3.2	EVP, 0 layers
Meteorological Research Institute (Japan)	MRI-CGCM	FD, 0 layers
Department of Energy (USA)	PCM	EVP

[1]same abbreviations as in Table 1. Number of layers refers to temperature layers in ice (and sometimes snow too). A 0-layer model assumes a linear temperature profile in the ice and snow as in Semtner (1976). A heat reservoir is for solar radiation as in Semtner (1976) and brine pockets as in Bitz and Lipscomb (1999) or Winton (2000).

warm the interior and expand brine pockets.

A sophisticated treatment of melt ponds was implemented in a single-column sea ice model quite some time ago (Ebert and Curry, 1993), and recently a melt pond model was extended

to also include a more consistent two-stream radiative transfer model through ice and ponds (Taylor and Feltham, 2004). Another new radiative transfer method for sea ice and ponds incorporates a Delta-Eddington, multiple-scattering radiative transfer approach to account for multiple scattering from snow grains, bubbles, and brine pockets (Briegleb and Light, 2007). Without a doubt climate modelers are taking note of these advances and some of these features will be incorporated in the next generation sea ice models, many of which are being developed for the next IPCC.

Of course the behavior of sea ice is closely tied to the atmospheric and oceanic boundary layers. Thus modeling sea ice depends fundamentally on the other components in a climate model and on the way the components are coupled. Table 3 summarizes what I consider to be major problems with sea ice modeling in global climate models in the 1990s and early 20th century, from the sea ice component alone or across components.

Table 3: Summary of issues with sea ice in CMIP2 global climate models in the late 1990s and an indication of whether they are fixed in the best 21st century CMIP3 models yet.

Older Model Issues	fixed yet?
Lack of reasonable sea ice dynamics	yes
Lack of ice thickness distribution	yes
Lack of brine pockets	yes
Biases in surface wind stress	partly
Biases in atmospheric fluxes	no
Biases in ocean heat transport	no
Lack of melt ponds	soon
Beer's law radiation[1]	soon
Ice-ocean exchange overly crude[2]	soon

[1]Beer's law should only be used for absorption in a semi-infinite medium, which is a poor approximation for sea ice where the surface albedo varies with thickess.
[2]For example, sea ice floes and ridges should be treated as actually embedded in the ocean and sea ice desalination should occur over many months.

1.2 Sea Ice Physics in Leading Climate Models

State of the art climate models today treat the jumble of sea ice floes as a continuum. Thus sea ice is generally described in terms of a distribution of sea ice thicknesses at the subgrid-scale. The ice motion is also considered for a continuum, rather than for individual floes. With this brief overview, a global-scale sea ice model can be conveniently developed from four governing equations.

Four Governing Equations

The best sea ice components in global climate models today explicitly compute the ice-thickness distribution (see Table 2). Among these models, the formulation of the sea ice

model begins with the ITD equation. The ITD is a probability density function (pdf), usually written $g(h)$, that describes the probability that the ice cover in particular region has thickness h. A cruder alternative is to model the mean thickness of the pdf and the total ice concentration.

In a sea ice model, the ITD describes the pdf of a grid cell and thus it is sometimes called a subgrid-scale parameterization. A parameterization typically represents processes that are too small-scale or complex to be represented explicitly. For example, deformation is parameterized with a set of rules[1] that select the portion of the ITD that will deform and then redistribute it within the ITD. In contrast, ice growth and melt alter the ITD in a way that is computed from first principles. Hence the ITD actually includes both parameterized and explicit physics.

The ITD equation is

$$\underset{1}{\frac{Dg}{Dt}} = \underset{2}{-g\nabla\cdot\mathbf{u}} + \underset{3}{\Psi} - \underset{4}{\frac{\partial}{\partial h}(fg)} + \underset{5.}{\mathcal{L}} \tag{1}$$

Term 1 is the Lagrangian derivative of g following an ice "parcel", term 2 is the rate of change of g from parcel convergence, term 3 is the mechanical redistribution (see Fig. 1), term 4 is the advection of g in ice-thickness space from growth/melt (see Fig. 2), and term 5 is the reduction rate of g from lateral melt. Here, $\mathbf{u}$ is the ice velocity and f is the net growth rate. The ITD equation was introduced by Thorndike et al. (1975). Models that specify the ITD (e.g. Walsh et al., 1985) or only permit a single ice thickness in the ice covered fraction of a model grid cell (e.g. Hibler, 1979), would have an equation for the gridcell mean ice thickness instead.

There are two parts to deformation: a rate of opening (creating open water) and closing (closing open water and/or deforming and redistributing the ice), which depend on $\mathbf{u}$, and a redistribution process (or ridging mode), which depends on $g(h)$. The opening and closing rates depend on the convergence and/or shear in the ice motion field. It may not be obvious that shear would cause deformation. Imagine that the ice pack is composed of pieces with jagged edges. When shearing, the jagged edges can catch on one another and cause deformation, which converts kinetic energy into potential energy from piling up ice, or shearing can cause frictional loss of energy and no deformation. Thus the closing rates also depend on assumptions made about frictional losses, see e.g., (Flato and Hibler, 1992; Bitz et al., 2001).

For the redistribution process, some portion of the ITD is identified as potentially able to "participate" in redistribution (see Fig. 1). A typical rule assumes only the thinnest 15% of the ITD participates. If the open water fraction exceeds 15%, then no redistribution takes place, and instead the open water closes under convergence and nothing happens under shear. This participation function is weighted according to its thickness, so that the thinnest ice is most likely to deform. Another rule is needed to redistribute the ice that ridges. Originally, Thorndike et al. (1975) proposed that ice that ridges would end-up five times thicker than

[1]Deformation can be treated from first-principles in finite element models (e.g., Hopkins and Hibler, 1991; Hopkins, 1996), but there is no differential equation that describes deformation in a model composed of gridcells, as in climate models. At the moment, finite element models of sea ice have not been implemented in climate models.

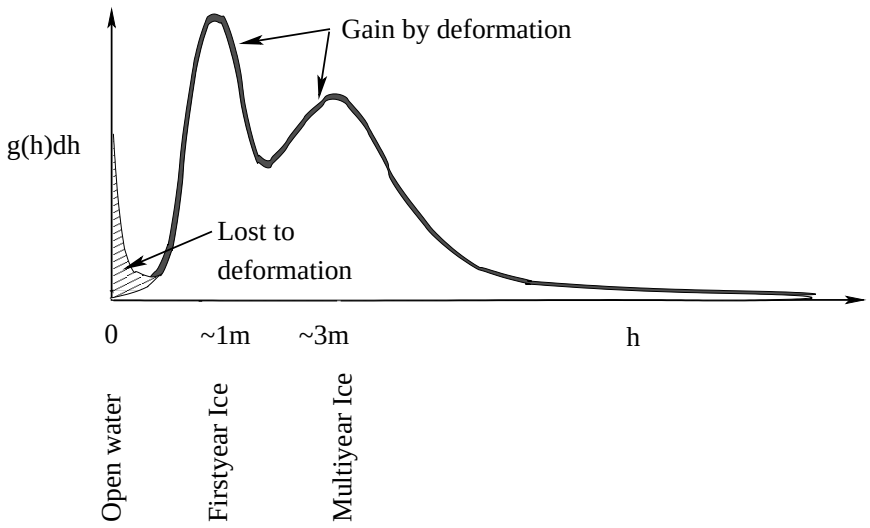

Figure 1: Illustration of deformation. The portion of the distribution labeled "lost to deformation" is also known as the ice that participates in redistribution. It subsequently is redistributed to thicker parts of $g(h)$, where it is labeled "gain by deformation".

its starting thickness. Other more complex redistribution schemes have been used since then (e.g., Hibler, 1980; Lipscomb et al., 2007).

Ice growth or melt causes $g(h)$ to shift along its x-axis, or thickness space. This process is illustrated in Fig. 2. The growth/melt rate depends on thickness, so $g(h)$ becomes distorted in the process.

The second governing equation is conservation of momentum:

$$\underset{1}{m\frac{D\mathbf{u}}{Dt}} = \underset{2}{-mf\mathbf{k}\times\mathbf{u}} + \underset{3}{\boldsymbol{\tau}_a} + \underset{3}{\boldsymbol{\tau}_w} \underset{4}{- mg_r\nabla Y} + \underset{5.}{\nabla\cdot\sigma} \tag{2}$$

Term 1 is the Lagrangian derivative of $\mathbf{u}$ following an ice parcel, term 2 is the Coriolis force, terms 3 are the air and water stresses, term 4 is the force due to ocean surface tilt, and term 5 is the ice internal force, where m is mass per unit area, f is the Coriolis parameter, g_r is gravity, Y is the sea surface height, and σ is the ice stress.

A constitutive law characterizes the relationship between the ice stress and strain rate and defines the nature of the ice dynamics (e.g., VP, CF, or EVP). A simplistic picture of a converging ice pack with uniform thickness under an imposed compressive wind force is given in Fig. 3. Sea ice generally repels a compressive force somewhat, even if it is deforming. The resulting internal force is associated with a nonzero stress state. In Fig. 3 the ice pack is converging such that its length L on one side decreases by δL in some time δt, so the ice experiences a strain $\epsilon = \delta L/L$ and a strain rate $\dot{\epsilon} = \delta L/L\delta t$. A modeler chooses the constitutive law to relate σ and $\dot{\epsilon}$, which are actually two-dimensional tensors, not scalars as I have shown here for illustrative purposes only. Other chapters in the volume describe sea ice dynamics in far greater detail.

Conservation of enthalpy E (the energy required to melt sea ice) is the third governing

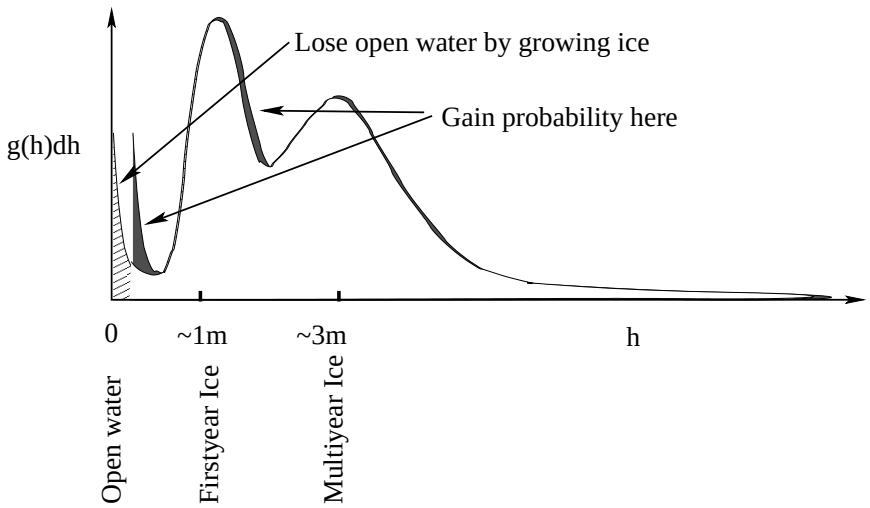

Figure 2: Illustration of advection in thickness space.

equation:

$$\underset{1}{\frac{DE}{Dt}} = \underset{2}{E\nabla \cdot \mathbf{u}} + \underset{3}{\Pi} + \underset{4.}{\mathcal{E}} \tag{3}$$

Term 1 is the Lagrangian derivative of E following an ice parcel, term 2 is the rate of change to E from parcel convergence, term 3 is the mechanical redistribution of E, and term 4 is the rate of change to E from thermodynamics.

The fourth and final governing equation is the heat equation in ice and snow:

$$\underset{1}{\rho c \frac{\partial T}{\partial t}} = \underset{2}{\frac{\partial}{\partial z} k \frac{\partial T}{\partial z}} + \underset{3.}{Q_{\mathrm{SW}}(z)} \tag{4}$$

Term 1 is the thermal energy change in a layer at some location, term 2 is the gradient of the conductive flux, and term 3 is the absorption of solar radiation. Here, ρ is the density, c is the heat capacity, and k is the conductivity. A heat equation for sea ice that takes into account brine pockets by making c and k functions of temperature and salinity was introduced by Maykut and Untersteiner (1971) and will be described below.

The heat equation is partly responsible for the $\mathcal{E}$ in Eq. 3. Growth and melt also influence $\mathcal{E}$. I do not include equations for growth and melt in my set of governing equations. I discuss them when I discuss brine-pocket physics in the next section.

I have not yet described an explicit conservation equation for ice volume (or mass) because conservation of volume is contained in the equation for $g(h)$ (or at least it depends on the way $g(h)$ is discretized). I also have no equation for the salinity of sea ice, because it is time-independent in all but one or two climate models at this time. In a few years I hope models will include desalination in the set of governing equations in a physically correct manner.

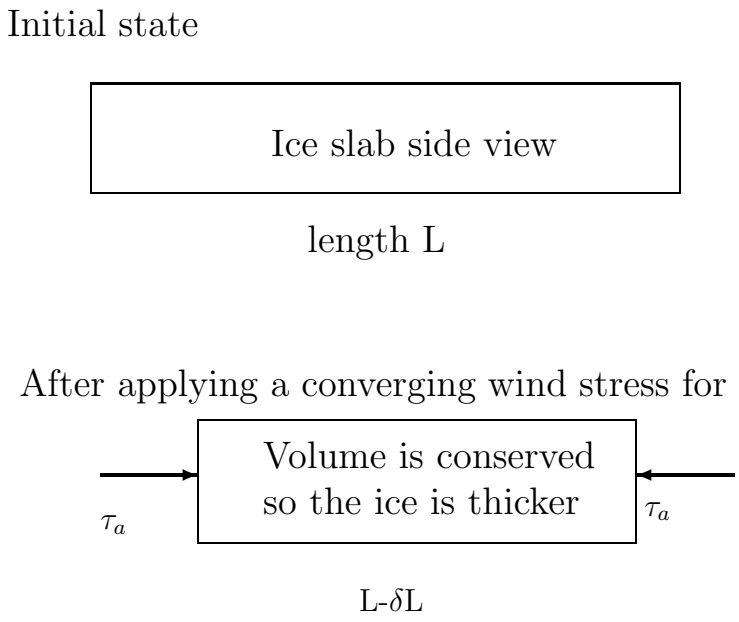

Figure 3: Illustration of ice slab that deforms under compressive force.

Sea ice thermodynamics with explicit brine-pockets

In this section I describe the thermodynamics of a sea ice model with explicit brine-pockets. Various simplifications to the method I described have been used. However, the full physics are elegant, straightforward, and fairly easy to implement. Section 2 describes a sea ice thermodynamic modeling exercise that was given at the Svalbard sea ice summer school in July, 2006. The model used in section 2 is based on the equations that follow.

Untersteiner (1961) proposed an equation for the heat capacity of sea ice to take into account the thermal inertia of brine pockets as

$$c(T, S) = c_o + \frac{\gamma S}{T^2}, \tag{5}$$

where c_o is the heat capacity of fresh ice, S is the salinity in parts per thousand (‰), and T is the temperature in Celsius. Untersteiner fit γ to the values of heat capacity tabulated by Malmgren (1927) and also suggested a formula for the sea ice conductivity $k(S, T)$.

Later, Ono (1967) pointed out that Eq. (5) can be derived from first principles such that

$$\gamma = L_o \mu \tag{6}$$

where L_o is the latent heat of fusion of fresh ice, at 0° C and μ is an empirical constant from the linearized relationship between the melting temperature and salinity of sea ice, $T_m = -\mu S$.

Equation (5) can be multiplied by the sea ice density and integrated to give the amount of energy Q required to raise the temperature of a unit volume of sea ice from T to T':

$$Q(S, T, T') = \rho c_o (T' - T) - \rho L_o \mu S \left(\frac{1}{T'} - \frac{1}{T} \right). \tag{7}$$

When $T' = T_m$ a unit volume of sea ice should consist entirely of brine; that is, the melting is complete. Thus $Q(S, T, T_m)$ is the amount of energy needed to melt a unit volume of sea ice of salinity S at temperature T, or

$$q(S,T) = \rho c_o (T_m - T) + \rho L_o \left(1 + \frac{\mu S}{T}\right), \tag{8}$$

which is the enthalpy per unit volume of sea ice (E is q times the volume).

For $S = 0$, q is what we would expect for pure ice: a heat capacity term equal to the energy required to raise the temperature to 0° C and a latent heat term equal to the energy required to melt the ice. Although q is undefined at 0° C, it is well behaved up to T_m, at which point $q = 0$ and the ice is completely melted. Hence, over the range of relevant temperatures, there is no singularity in (5) or (8). Fig. 4 illustrates the ratio of q to ρL_o as a function of T and S. These equations assume the density is constant, but an easily computed quantity $\rho(1 + \mu S/T)$ indicates the mass of brine per unit volume of sea ice.

Bitz and Lipscomb (1999) pointed out the importance of taking into account brine pockets when computing ablation and accretion:

$$F(T) = -q(S,T)\frac{dh}{dt}, \tag{9}$$

where F is the net flux toward the top or bottom surface, h is the ice thickness, and t is time. They also explained an energy-conserving solution to the heat equation was easily achieved by integrating the heat equation:

$$Q(T, T') = \int_t^{t+\Delta t} \left(\frac{\partial}{\partial z} k \frac{\partial T}{\partial z} + Q_{\mathrm{SW}}(z)\right) dt \tag{10}$$

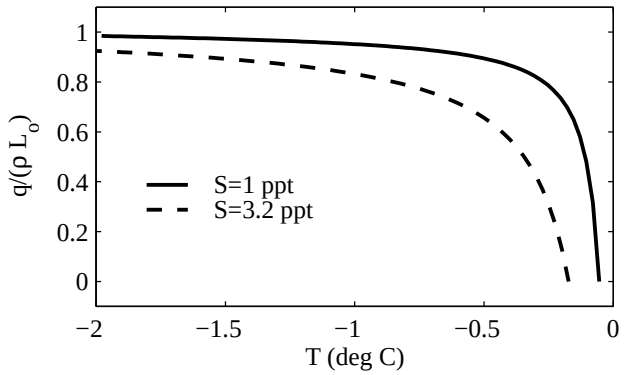

Figure 4: Energy of melting relative to the latent heat of fusion of pure ice as a function of temperature for $S = 3.2‰$ and $S = 1‰$.

Nearly all models that treat brine pockets explicitly prescribe a time invariant vertical salinity profile $S(z)$ that resembles measurements of perennial sea ice after it has been well-flushed with snow melt. This is not well justified, but it is practical at this time.

The evolution of the ice plus brine system that makes up sea ice has been related to mushy layer theory from material science (e.g., Feltham and Worster, 1999). In the limit that the

salinity profile is fixed in time, Feltham et al. (2006) show that the mushy layer theory is equivalent to the heat-capacity Eq. 5 introduced by Untersteiner (1961). It is also equivalent to the sea ice enthalpy as described here. Notz and Worster (2006) incorporate salinity flushing in a sea ice model of the mushy layer equations but did not yet account for gravity drainage, the major souce of desalination during winter (Notz and Worster, 2009). Notz and Worster note that that their model is also unfortunately still too computationally expensive for large-scale climate modeling.

Discretization of the Ice Thickness Distribution

The ice-thickness distribution can be discretized in a number of ways. The ITD models that were first designed for basin-scale (or larger) studies assume g(h) is distributed uniformly between each category boundary (Hibler, 1980; Flato and Hibler, 1995, e.g.,), as illustrated in Fig 5a. Consequently sea ice growth/melt requires a procedure known as advection in thickness-space, and the method of resolving the thickness distribution can be termed Eulerian. Advection in thickness-space causes diffusion among categories, which can be reduced by resolving many thickness categories. An advantage of the method is its simplicity, as only the concentration is needed to describe a thickness category, because the mean thickness of a category is always at the midpoint between category boundaries.

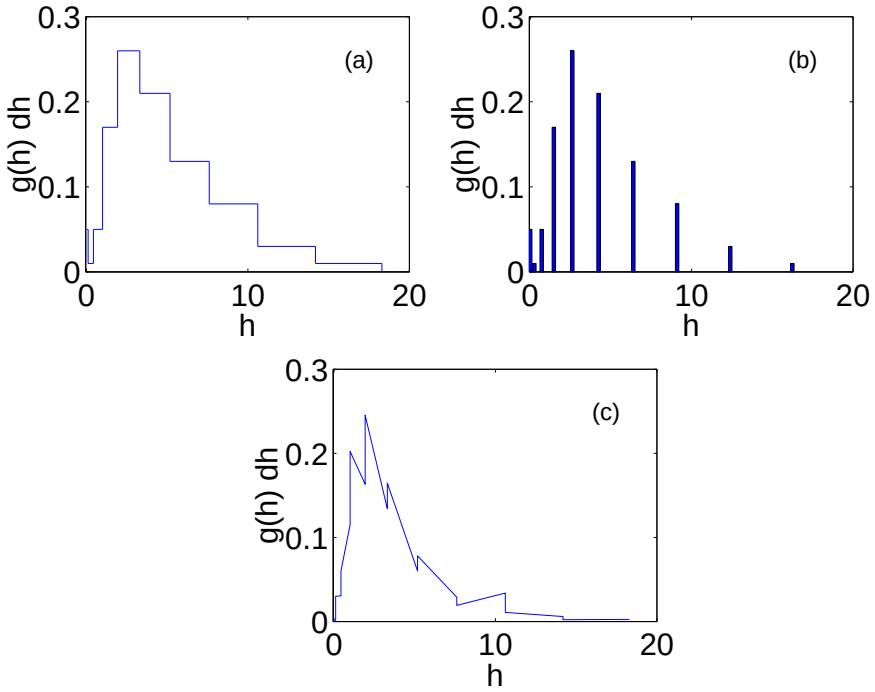

Figure 5: Various discretizations proposed for $g(h)$ (a) constant between category boundaries (Hibler, 1980), (b) a series of δ-functions that move in thickness space (Thorndike et al., 1975; Bitz et al., 2001), and (c) piecewise continuous with linear functions between category boundaries (Lipscomb, 2001).

Thorndike et al. (1975) originally formulated a model where the ice in each category is variable in thickness (see 5b). This discretization is Lagrangian in thickness-space and it is

free of the diffusion associated with thickness advection in Eulerian models. The trade-offs are (1) categories are defined by concentration and thickness and (2) something must be done to limit the number of ice thickness categories when processes such as growth over open water and ridging create new thicknesses of ice. Thorndike et al. (1975) suggested interpolating the ITD to a grid fixed in thickness space at each time step, which turns out to be a very diffusive process. Bitz et al. (2001) implemented a Lagrangian ITD in a global climate model but instead constrained each category to lie between thickness boundaries. When a category outgrows its limits, the ice was transfered from one category to another. Bitz et al. (2001) showed that about five categories of sea ice was sufficient to capture most of the behavior that is needed in a climate model, and further showed that with just five categories it is reasonable to include sophisticated thermodynamics with brine-pocket physics.

Lipscomb (2001) introduced a discretization for $g(h)$ that is piecewise continuous with linear functions between category boundaries (see Fig. 5c) and can be considered intermediate to those in Fig. 5 a and b. The linear functions vary with growth and melt and the evolution of $g(h)$ owing to growh or melt is more accurate than for a $g(h)$ that is a series of δ-function and less diffusive than the $g(h)$ that is constant between boundaries. However, all three method treat $g(h)$ as a series of δ-functions with regard to deformation and redistribution.

A possible set of state variables

A possible set of state variables for each category i of a sea ice model in a global climate model is A_i, V_i, V_i^s, $E_i(z)$, and $E_i^s(z)$ where:

A_i is the category area per unit gridcell area (or fractional coverage)

$V_i = h_i A_i$ is the category volume per unit gridcell area

$E_i = V_i q_i$ is the category enthalpy per unit gridcell area

The superscripted s indicates snow, and no superscript indicates sea ice. The set must also include any other variables that describe the evolution of the surface state, such a melt pond depth and area. Finally the velocity $\mathbf{u}$ is also a state variable, and it alone has no category index because it is the same for the whole grid cell.

I prefer to use conserved quantities as state variables, which is why my set doesn't include h_i or $T_i(z)$. This way each state variables except $\mathbf{u}$ can be solved from a continuity equation (e.g., Eq. 3).

Computation Time

Computation time given to the sea ice component of a typical climate models is roughly 10-20%, although it could easily be more or less depending on the relative resolution, sophistication, and optimization among components. Arguably, the sea ice component is a modest computation expense for most climate models and claims that sea ice physics are kept crude to reduce computation costs should be met with skepticism. A more likely explanation is

that the human resources needed to construct and manage a high-quality sea ice model have been directed elsewhere.

The computation time for sea ice in the CCSM3 is about 15% when the model is run with 2.8° resolution in the atmosphere and land and nominally 1° resolution in the ocean and sea ice. Of the time devoted to the sea ice, about 2/3 is given to solving the equations describing the sea ice and 1/3 is given to coupling and input/output. Of the 2/3 given to sea ice equations:

- 55% is for the EVP dynamics,
- 19% is for thermodynamics with four vertical layers and brine-pocket physics
- 15% is for advection with the incrementing remapping algorithm, and
- 11% is for mechanical redistribution

This model was run with five ice-thickness categories.

A key consideration for climate modelers is to design a model that can run the scenarios of interest in a time to meet publication deadlines. Choices must be made to balance model resolution, physics, parameterizations, and numerics. High performance computers today have tens of thousands of cores and many have been constructed for the purpose of running climate models. Codes must parallelize well to take advantage of these machines, and sea ice codes generally do because there are relatively many schemes that operate at the grid-scale (e.g., vertical heat equation) and subgrid-scale (e.g., deformation). The Los Alamos Sea Ice CICE has already been successfully scaled beyond 10,000 cores on Cray XT equipment (Dennis and Tufo, 2008).

1.3 Conclusions

Climate model resolution is nearing the large floe-scale, where sea ice can no longer be considered a continuum. I expect some climate models will adopt non-continuum sea ice dynamics in the 5-10 yr timeframe to break the floe-scale resolution limit. In the next 5 years, I expect the major new physics to be added to sea ice models will be explicit melt ponds; better radiative transfer and snow morphology; and primitive salinity, fluid transport, and biogeochemistry. The greatest computational increase could be to advect many new variables if it weren't for schemes such as incremental remapping which can efficiently transport large numbers of sea ice state variables (Lipscomb and Hunke, 2004). Computational resources will not be the limiting factor to implementing these new features. Instead, expertise in sea ice and polar climate at the modeling centers and errors in the other climate model components will limit advances. Learning how sea ice models in today's global climate models work is the first step to meet this certain need.

2 Exercises Using a Thermodynamic Sea Ice Model

In this section you will be guided through exercises given at the summer school that allow you to explore the sensitivity of sea ice thickness to climate forcing perturbations and to model parameters. The exercises use the single-column, thermodynamic sea ice model that is described in section 1.2. A more complete description can be found in Bitz and Lipscomb (1999). Following the exercises is a discussion of the expected results. The exercises are designed to give you a thought provoking research experience, rather than a crank-turning, answer-driven experience.

Sea ice is modeled as a motionless single slab, with no open water fraction. The ice temperature is resolved in 10 layers, and brine pockets are parameterized explicitly with a temperature and salinity dependent heat capacity and conductivity, following Maykut and Untersteiner (1971). This model also takes into account the internal melt in brine pockets when computing ablation at the top and bottom surfaces. The atmospheric model forcing is from the standard case in Maykut and Untersteiner (1971), which is based on the work of Fletcher (1965). The surface albedo is 0.63 for bare ice, 0.75 for wet snow, and 0.80 for dry snow.

The model is composed of 10 MATLAB scripts and one data file. You will need access to a computer with MATLAB. The model may be downloaded as a tarfile from http://www.atmos.washington.edu/∼bitz/column.tar (untar by typing *tar xvf column.tar*), or as individual files from http://www.atmos.washington.edu/∼bitz/column/.

First familiarize yourself with the model, by running it once with the default parameters and forcings by typing *column* in the MATLAB command window. When it is finished, type *help column* in the same window to learn how to vary the model options.

2.1 Exercises

Part 1 Investigate the model sensitivity to varying the downward longwave radiative flux F_{LW}. Perturb the downward longwave flux (i.e., F'_{LW}) all year through the function call list (e.g., type *column(-2)*) and make a table of the corresponding annual mean thickness $\bar{h}$ and mean February-March surface temperature T_{FM} in the final year of the run (the model displays these statistics in the command window). If necessary, increase the number of run years so the model reaches an approximate equilibrium by the time it finishes. Vary F_{LW} between +/-10 W m^{-2} in increments of about 2W m^{-2}, but do not reduce F_{LW} so much that the snow does not melt in summer. Plot T_{FM} as a function of $\bar{h}$.

Options to considers

1) Why does the time to reach equilibrium vary?

2) Why is the plot of $T_{\mathrm{FM}}(\bar{h})$ nonlinear?

3) Using a hierarchy of models can be useful for understanding model results. Even this thermodynamic sea ice model is quite complex. You are encouraged to try to relate your results to an analytical model of sea ice. One such model is Thorndike's toy model (Thorndike, 1992) with the following basic relations:

Winter Energy Balance

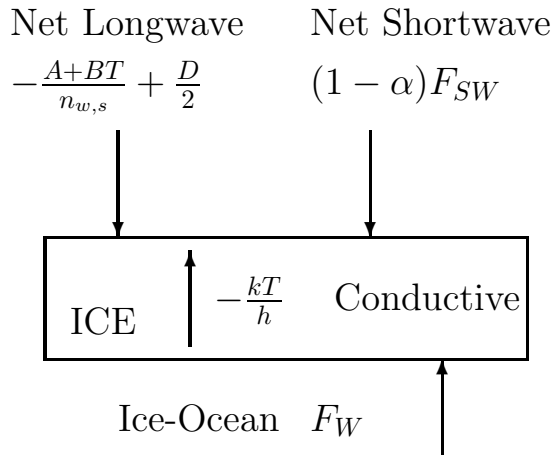

Figure 6: Heat fluxes in a sea ice slab.

The flux balance at the top surface from Fig. 6 is

$$F_{\mathrm{LW}} - (A + BT_s) = \frac{kT_s}{h}, \tag{11}$$

where surface outgoing longwave $\epsilon\sigma T_s^4$ is approximated as $A + BT_s$, turbulent heat fluxes are neglected, and the temperature profile in the ice is assumed to be linear.

The equation may be simplified to

$$W - BT_s = \frac{kT_s}{h}, \tag{12}$$

Solve Eq. 12 for $h(T_s)$ and assume this equation can be related to $\bar{h}(T_{\mathrm{FM}})$, and plot it on the curve you created with output from the MATLAB model. Use the following parameters: $W = -160\mathrm{W\ m^{-2}}$, $B = 4.6\mathrm{W\ m^{-2}\ (deg\ C)^{-1}}$, and $k = 2\ \mathrm{W\ m^{-1}\ (degC)^{-1}}$, to give you h in meters (not centimeters as in the MATLAB model).

Annual Energy Balance

Figure 6 also applies in summer, except the net shortwave is not zero and the surface temperature is assumed to be zero Celsius. When the ice reaches an equilibrium thickness, the annual heat input into the ice must be zero. In the spirit of Thorndike (1992), let

$$\tau_{\mathrm{W}}(W - BT_s) + \tau_{\mathrm{S}}S + (\tau_{\mathrm{W}} + \tau_{\mathrm{S}})F_w = 0 \tag{13}$$

where T_s is from the winter season, S is the net downward radiative flux in summer, $\tau_{\mathrm{W,S}}$ is the length of the winter or summer (and no other seasons exist). After substituting from the winter energy balance, we arrive at

$$\tau_{\mathrm{W}}(kT_s/h) + \tau_{\mathrm{S}}S + (\tau_{\mathrm{W}} + \tau_{\mathrm{S}})F_W = 0, \tag{14}$$

F'_{LW} W m^{-2}	$\bar{h}$ m	T_{FM} deg C	$\delta h/\delta F_{\mathrm{LW}}$ cm W^{-1} m^2
-4	620	-33.7	120
-2	380	-32.5	58
0	264	-31.4	35
2	195	-30.3	25
4	145	-29.3	18
6	109	-28.3	15
8	80	-27.6	

Table 4: Results from varying downward longwave flux with the model.

Solve for $T_s(h)$ and plot it on your figure. Use $S = 22\mathrm{W\ m^{-2}}$, $F_W = 2\mathrm{W\ m^{-2}}$ and for simplicity $\tau_{\mathrm{W}} = \tau_{\mathrm{S}}$. The intersection of the two analytical expression from the toy model gives an approximate solution to the Thorndike toy model.

Part 2 A climate modeler faced with biases in their model will often tune the surface albedo. This question invites you to explore some of the consequences. Find two different combinations for F_{LW} and surface albedo α that give roughly the same T_{FM}, $\bar{h}$ state. Vary α (0.05 is sufficient) by editing the script "calc_albedo.m" and vary F_{LW} from the function call list. Be sure to apply the same perturbations year round.

Now perturb the downward longwave further by $\delta F_{\mathrm{LW}} = 2\mathrm{W\ m^{-2}}$ for each F_{LW}, α pair and find the thickness sensitivity $\delta h/\delta F_{\mathrm{LW}}$. Do they differ substantially? Why or why not?

Compute $\delta h/\delta F_{\mathrm{LW}}$ for your MATLAB runs from part 1 and note that it varies considerably. Why?

Part 3 How do F_{LW} perturbations in winter or summer only affect the ice thickness? Design your own experiments to investigate this question. Type *help column* in the matlab command window to find a quick way to perturb F_{LW} in winter or summer only. The time of year when downward longwave has the most spread among models is winter, because climate models have large spread in their simulation of wintertime cloud fraction.

2.2 Exercise results and discussion

Part 1

Your work from part 1 should result in numbers like those in table 4 (ignore the last column for now). Yours may differ slightly, depending on how well equilibrated the model was when it finished.

$\bar{h}$ vs T_{FM} is plotted in Fig. 7 with the curves for $h(T)$ and $T(h)$ from Eqs. 12 and 14. The solid line is deceptively close to the circles, but it should not lie on top of them. Instead the intersection of the pair of lines should roughly intersect at one of the circles. In principle, we could vary the longwave flux and estimated a series of intersecting lines that should each approximately intersect at a circle, but that would make for a messy plot. The analytic

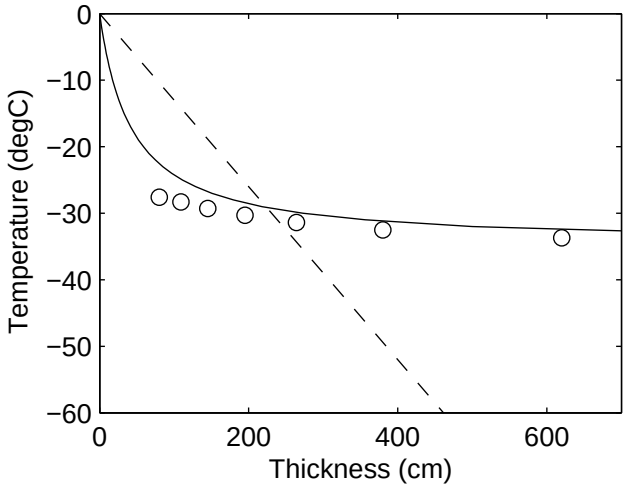

Figure 7: $T_{\rm FM}$ versus $\bar{h}$ from table 4 (circles) with curves for $h(T)$ (solid line) and $T(h)$ (dashed line) from Eqs. 12 and 14, respectively.

model is meant to show you how fluxes must be in balance to yield an equilibrium thickness and temperature yearround. When the ice thickness is not at equilibrium, the thickness and temperature state in late winter will still lie on the solid curve, but that state will not intersect the dashed curve. In this case the annual net flux balance will not be met and the ice will either grow or melt owing to the imbalance. The system adjusts by moving along the solid line until it intersects the dashed line, where the annual net flux into the ice is zero.

You should have found that larger $\bar{h}$ runs take longer to equilibrate. For a slab of ice, neglecting the effect of open water, the equilibration time depends on how much a small change in thickness results in a change in ice growth (Untersteiner, 1961) (or conduction through the ice). You can see this if you look closely at Fig. 8a, which is a run with $F'_{\rm LW} = 4$ W m^{-2}. Which varies more over time during the run, the amount of growth in winter or amount of melt in summer? At the beginning of the run, the ice grows about 50 cm yr^{-1} and melts about 65 cm yr^{-1}. To reach equilibrium the growth must catch up with the melt, and by the end of the run, growth and melt are about 78 cm yr^{-1}. The imbalance causes the ice to thin. The growth rate adjusted fairly quickly because a fairly small change in thickness resulted in a big change in growth and a smaller change in melt. In turn, this quick adjustment reduces the imbalance quickly.

Now look at at Fig. 8b, which is a run with $F'_{\rm LW} = -4$ W m^{-2}. At the beginning of the run, the ice grows about 47 cm per year but only melts about 33 cm yr^{-1}. (Notice that the ice growth is much more sensitive to thickness than to $F'_{\rm LW}$.) This time the ice growth must decrease to balance melt, and the imbalance causes the ice to thicken. However, the growth doesn't change very fast with time, and the ice takes a very long time to reach equilibrium. After 20 years the ice growth is still about 29 cm yr^{-1} and melt is about 23 cm yr^{-1}.

We can estimate the equilibration timescale from the following relation

$$\text{timescale } = \left(\frac{\partial G}{\partial h} - \frac{\partial M}{\partial h} \right)^{-1}$$

where G is the amount of growth that occurs in winter and M is the amount of melt that

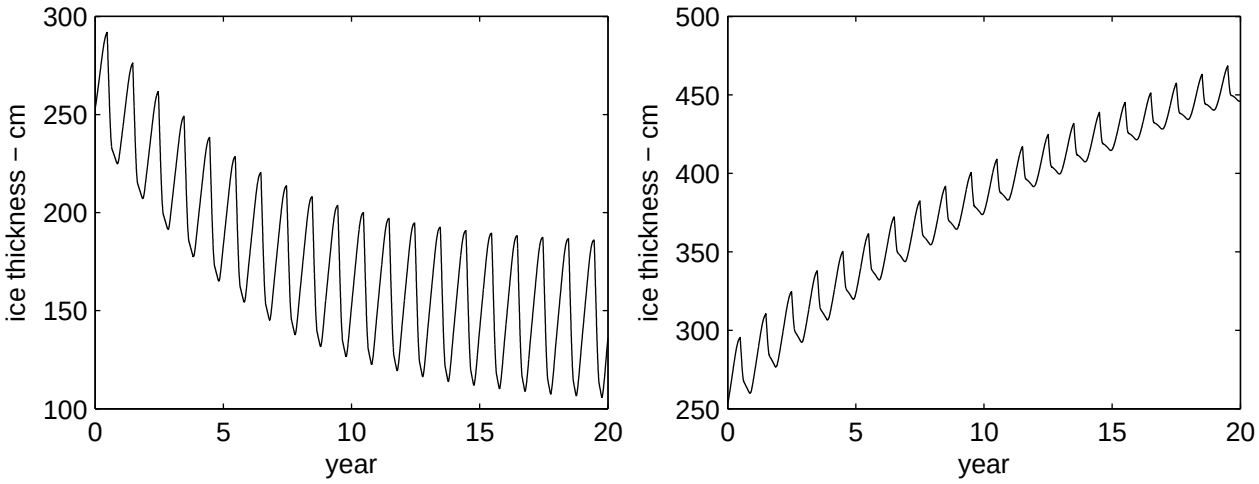

Figure 8: Ice thickness adjustment for first 20 years of runs with (a) $F'_{\mathrm{LW}} = 4$ W m^{-2} and (b) $F'_{\mathrm{LW}} = -4$ W m^{-2}

occurs in summer. For simplicity neglect $\partial M/\partial h$, which is smaller than the $\partial G/\partial h$, and it is easier to see that the the inverse of the rate of change of the growth with thickness roughly sets the equilibrium timescale. The growth rate of sea ice depends on the conductive flux through the ice, which is inversely proportionate to its thickness. Hence small ice thickness changes result in much greater growth changes for thin ice, say 1-2 m ice, compared to thicker ice, say 4-5 m ice.

As the thicker ice takes longer to equilibrate, it also changes much more for a given forcing perturbation (see the final column in table 4. You can read more about the relationship between sensitivity, timescale, and thickness in Bitz and Roe (2004).

Part 2

You can recycle runs from part 1 with the default albedo and longwave flux. Then produce another run with about the same $\bar{h}$ but with 0.04 from the albedo of every surface type and the the downward longwave flux reduced by 8 W m^{-2}, see table 5.

You could then rerun both of these cases but with the longwave flux increased by 2 W m^{-2}. The resulting thickness sensitivity $\delta h/\delta F_{\mathrm{LW}}$ is about the same for both, especially when compared with the large range that the runs in part 1 exhibit (see last column of table 4).

The main point of this exercise is that in the absence of open water and without a thickness-dependent albedo parameterization, tuning the albedo doesn't change the thickness sensitivity. In contrast, the mean ice thickness has an enormous effect on the thickness sensitivity. Tuning is a necessary part of climate modeling because of this extreme sensitivity to the mean ice thickness.

This model has ice-albedo feedback limited to the transition of dry to wet snow and then to bare ice. There is no explicit feedback as the ice thins or disappears, so this model is only appropriate to test the sensitivity of high concentration ice with thickness greater than about a meter. The thickness sensitivity to albedo changes would certainly be different for an ice cover with thin ice and open water. If you want to explore the thickness sensitivity with more varied ice cover, you must use a different model or alter this one.

α	F'_{LW} W m^{-2}	$\bar{h}$ m	$\delta h/\delta F_{\mathrm{LW}}$ cm W^{-1} m^2
default	0	264	35
default	2	195	
default - 0.04	-8	264	33
default - 0.04	-6	198	

Table 5: Results from varying albedo and downward longwave flux with the model.

Part 3

Your work from part 3 should result in numbers like those in table 6. It is quite clear that F_{LW} perturbations in summer have a greater influence on the ice thickness. This is some consolation to the fact that the biases in F_{LW} in climate models are worst in winter, not summer.

F'_{LW} W m^{-2}	season	$\bar{h}$ m	δh cm
0		264	
2	all year	195	69
2	winter	244	20
2	summer	212	42

Table 6: Results from varying downward longwave flux all year or for only winter or summer with the model.

For more practice. Think about the extent to which these exercises are applicable to global climate modeling. Try varying the sea ice salinity profile in the script salinity_prof.m or vary the albedo in summer only and repeat part 2.

References

Bitz, C. M., M. M. Holland, A. J. Weaver and M. Eby, 2001: Simulating the ice-thickness distribution in a coupled climate model. *J. Geophys. Res.*, **106**, 2441–2464.

Bitz, C. M. and W. H. Lipscomb, 1999: An energy-conserving thermodynamic model of sea ice. *J. Geophys. Res.*, **104**, 15,669–15,677.

Bitz, C. M. and G. H. Roe, 2004: A mechanism for the high rate of sea-ice thinning in the arctic ocean. *J. Climate*, **18**, 3622–31.

Brandt, R. E., S. G. Warren, A. P. Worby and T. C. Grenfell, 2005: Surface albedo of the Antarctic sea ice zone. *J. Climate*, pp. 3606–3622.

Briegleb, B. P. and B. Light, 2007: *A Delta-Eddington multiple scattering parameterization for solar radiation in the sea ice component of the Community Climate System Model*. NCAR/TN-472+STR.

Budyko, M. I., 1969: The effect of solar radiatin variations on the climate of the earth. *Tellus*, **21**, 611–619.

Dennis, J. M. and H. M. Tufo, 2008: Scaling climate simulation applications on the ibm blue gene/l system. *IBM Journal of Research and Development: Applications for Massively Parallel Systems*, **52(1/2)**, 117–126.

Ebert, E. E. and J. A. Curry, 1993: An intermediate one-dimensional thermodynamic sea ice model for investigating ice-atmosphere interactions. *J. Geophys. Res.*, **98**, 10085–10109.

Feltham, D. L., N. Untersteiner, J. S. Wettlaufer and M. G. Worster, 2006: Sea ice is a mushy layer. *Geophys. Res. Lett.*, **33, L14501**, doi:10.1029/2006GL026290.

Feltham, D. L. and M. G. Worster, 1999: Flow-induced morphological instability of a mushy layer. *J. Fluid Mech*, **391**, 337–357.

Flato, G. M. and W. D. Hibler, 1992: Modeling pack ice as a cavitating fluid. *J. Phys. Oceanogr.*, **22**, 626–651.

Flato, G. M. and W. D. Hibler, 1995: Ridging and strength in modelling the thickness distribution of Arctic sea ice. *J. Geophys. Res.*, **C9**, 18,611–18,626.

Fletcher, J. O., 1965: The heat budget of the Arctic Basin and its relation to world climate. Tech. Rep. R-444-PR, pp. 179, The Rand Corporation, Sant Monica, California.

Hibler, W. D., 1979: A dynamic thermodynamic sea ice model. *J. Phys. Oceanogr.*, **9**, 815–846.

Hibler, W. D., 1980: Modeling a variable thickness ice cover. *Mon. Wea. Rev.*, **108**, 1943–1973.

Holland, M. M. and C. M. Bitz, 2003: Polar amplification of climate change in the Coupled Model Intercomparison Project. *Clim. Dyn.*, **21**, 221–232.

Hopkins, M. A., 1996: On the mesoscale interaction of lead ice and floes. *J. Geophys. Res.*, **101**, 18315–26.

Hopkins, M. A. and W. D. Hibler, 1991: On the ridging of a thin sheet of lead ice. *Annals of Glaciology*, **15**, 81–86.

Hunke, E. C. and J. K. Dukowicz, 1997: An elastic-viscous-plastic model for sea ice dynamics. *J. Phys. Oceanogr.*, **27**, 1849–1867.

Lipscomb, W. H., 2001: Remapping the thickness distribution in sea ice models. *J. Geophys. Res.*, **106**, 13,989–14,000.

Lipscomb, W. H. and E. C. Hunke, 2004: Modeling sea ice transport using incremental remapping. *Mon. Wea. Rev.*, **132**, 1341–1354.

Lipscomb, W. H., E. C. Hunke, W. Maslowski and J. Jakacki, 2007: Improving ridging schemes for high-resolution sea ice models. *J. Geophys. Res.*, **112:C03S91**, doi:10.1029/2005JC003355.

Malmgren, F., 1927: On the properties of sea ice. in H. U. Svedrup, editor, *The Norwegian North Polar Expedition with the 'Maud' 1918–1925*, Vol. 1a, No. 5, pp. 1–67. Printed by John Griegs Boktr., Bergen, Norway.

Maykut, G. A. and N. Untersteiner, 1971: Some results from a time-dependent thermodynamic model of sea ice. *J. Geophys. Res.*, **76**, 1550–1575.

Meehl, G. A., G. Boer, C. Covey, M. Latif and R. Stouffer, 2000: Coupled Model Intercomparison Project. *Bull. Amer. Meteor. Soc.*, **81**, 313–318.

Meehl, G. A., C. Covey, T. Delworth, M. Latif, B. McAvaney, J. F. B. Mitchell, R. J. Stouffer and K. E. Taylor, 2007: The WCRP CMIP3 multimodel dataset: A new era in climate change research. *Bull. Amer. Meteor. Soc.*, pp. DOI:10.1175/BAMS–88–9–1383.

Notz, D. and M. G. Worster, 2006: A 1-d enthalpy model of sea ice. *Ann. Glaciol.*, **44**, 123–128.

Notz, D. and M. G. Worster, 2009: Desalination processes of sea ice. *J. Geophys. Res.*, p. submitted.

Ono, N., 1967: Specific heat and heat of fusion of sea ice. in H. Oura, editor, *Physics of Snow and Ice*, Vol. I, pp. 599–610. Institute of Low Temperature Science, Hokkaido, Japan.

Perovich, D. K. and Coauthers, 1999: Year on ice give climate insights. *EOS, Trans., Amer. Geophys. Union*, **80**, 481,485–486.

Sellers, W. D., 1969: A global climate model based on the energy balance of the earth-atmosphere system. *J. Appl. Meteor.*, **8**, 392–400.

Semtner, A. J., 1976: A model for the thermodynamic growth of sea ice in numerical investigaions of climate. *J. Phys. Oceanogr.*, **6**, 379–389.

Shine, K. P., A. Henderson-Sellers and R. G. Barry, 1984: Albedo-climate feedback: The importance of cloud and cryosphere variability. in A. L. Berger and C. Nicolis, editors, *New perspectives in climate modeling*, pp. 135–155. Elsevier, Amsterdamm, p 135-155.

Taylor, P. D. and D. L. Feltham, 2004: A model of melt pond evolution on sea ice. *J. Geophys. Res.*, **109, C12007**, doi:10.1029/2004JC002361.

Thorndike, A. S., 1992: A toy model linking atmospheric thermal radiation and sea ice growth. *J. Geophys. Res.*, **97**, 9401–9410.

Thorndike, A. S., D. S. Rothrock, G. A. Maykut and R. Colony, 1975: The thickness distribution of sea ice. *J. Geophys. Res.*, **80**, 4501–4513.

Untersteiner, N., 1961: On the mass and heat budget of arctic sea ice. *Arch. Meteorol. Geophys. Bioklimatol., A*, **12**, 151–182.

Walsh, J. E., W. D. Hibler and B. Ross, 1985: Numerical simultion of northern hemisphere sea ice variability 1951-1980. *J. Geophys. Res.*, **90**, 4847–4865.

Winton, M., 2000: A reformulated three-layer sea ice model. *J. Atmos. Ocean. Technol.*, **17**, 525–531.

Zhang, J. and W. D. Hibler, 1997: On an efficient numerical method for modeling sea ice dynamics. *J. Geophys. Res.*, **102**, 8691–8702.